

Journal of Nanophotonics

SPIEDigitalLibrary.org/jnp

Optical determination of thick graphene layer number based on surface plasmon resonance

Sherif H. El-Gohary
Nak-Hyeon Kim
Kyung Min Byun



Optical determination of thick graphene layer number based on surface plasmon resonance

Sherif H. El-Gohary, Nak-Hyeon Kim, and Kyung Min Byun

Kyung Hee University, Department of Biomedical Engineering, Yongin 446-701,

Republic of Korea

kmbyun@khu.ac.kr

Abstract. An optical method of measuring the number of layers in a graphene sample is formulated and compared with the conventional surface plasmon resonance (SPR) detection scheme, the latter being appropriate only for a very few graphene layers. Numerical results based on transfer-matrix method support that an alternative method, wherein the SPR substrate includes a dielectric overlayer, is feasible over a wide range of graphene layer numbers. While the multilayer graphene may lead to a broad and shallow SPR curve owing to the nonzero imaginary part in its relative permittivity, the dielectric overlayer makes the resonant surface plasmons less affected by graphene, resulting in a strong and deep absorption band at resonance. Linear regression analysis shows that the measurable graphene layer number can be as high as 50. © 2013 Society of Photo-Optical Instrumentation Engineers (SPIE) [DOI: [10.1117/1.JNP.7.073799](https://doi.org/10.1117/1.JNP.7.073799)]

Keywords: graphene layer number; surface plasmon resonance; dielectric overlayer; transfer-matrix method.

Paper 13042SS received Jun. 4, 2013; revised manuscript received Aug. 2, 2013; accepted for publication Aug. 7, 2013; published online Aug. 30, 2013.

1 Introduction

The unique properties of graphene sheets and their promising applications have been the objective of intensive research¹ since the successful isolation of single atomic planes of graphite in 2004.² Recently, graphene combined with surface plasmons has drawn a growing interest because of the potential that this two-dimensional (2-D) sheet of carbon atoms can provide new perspectives in plasmonics in various ways, such as a substrate which directly supports surface plasmons at infrared frequencies, a tunable transparent platform whose optical properties can be tuned by an external electric field, and a functional coating for the existing plasmonic devices.^{3,4}

As one example, we recently reported that surface plasmon resonance (SPR) biosensors with a graphene-on-silver substrate can be used to achieve a dramatically enhanced imaging sensitivity as well as to prevent silver film oxidation.⁵ A silver substrate with a few graphene layers was found to increase the imaging sensitivity significantly compared to a traditional gold-film-based SPR system. Also, the protective feature is attributed to the fact that when graphene layers are deposited on a silver film, the electron density of hexagonal rings is substantial enough to prevent atoms and molecules from passing through the ring structure,⁶ therefore, resulting in no reaction between oxygen gases and silver film. In such applications, an exact thickness measure of multilayer graphene is critical for manipulating and optimizing the thickness-dependent performance of the proposed systems.^{7,8}

Several optical techniques for counting the number of graphene layers have been proposed as candidates to overcome the limitation of conventional measure by atomic force microscopy (AFM).⁴ An AFM-based technique inherently suffers from an uncertainty because of the unknown gap thickness between neighboring graphene layers. On the other hand, while optical layer number determination by Raman scattering signal has been well established,^{9,10} it is still confronted with extrinsic effects such as impurities, defects, and optical configurations of the substrates^{11,12} as well as low throughput.¹³ More recently, optical detection based on SPR angle

shift, which corresponds to an increasing number of graphene sheets was proposed by Cheon et al. as a robust and quantitative approach.¹⁴ Although this SPR-based technique does not require a single-layer graphene substrate as a reference (as in Raman), the gold-film-based traditional SPR substrate was successful only for few graphene layers (<5) due to a broad and shallow SPR curve characteristic.

Moreover, the following key issues have not been addressed for the SPR-based graphene layer number counting: (1) Is the SPR substrate effectively applicable to a very thick graphene layer? It should be demonstrated that a large number of graphene layers are optically detectable in a reliable way. (2) What is the optimal structure that can provide a narrow and deep SPR curve? A significant number of graphene sheets will make the SPR curve broader and shallower and consequently lead to aggravation of sensing performance. (3) Does the SPR signal show a linear shift in a wide range of the graphene layer number? Together with a high sensitivity, a great linearity is essential for accurate determination of graphene layer thickness.

Although recent graphene research mainly has focused on the single- and double-layered sheets, we believe that multiple layers of graphene also have interesting aspects as they still exhibit unique 2-D properties.¹ Hence, this study is intended to propose an alternative, but effective, SPR structure for an accurate thickness determination of graphene layers, especially with a large layer number, by applying an intermediate dielectric layer between the gold film and graphene. Our suggestion is inspired by previous results which demonstrated that the SPR signal was significantly improved by employing metal-dielectric double-layered nanogratings.¹⁵ Such enhancement, compared with a single-layered metallic grating, was primarily due to the fact that the dielectric spacer can prevent the propagating surface plasmons from being interfered with by the locally enhanced fields excited at the gold nanogratings, finally resulting in a strong and deep absorption band. In this paper, it is expected that the dielectric overlayer will reduce the deterioration of plasmon waves by a highly absorptive graphene sheet. Thus, our study will serve as the first step to show the feasibility of dielectric-on-metal substrate for an accurate measurement of multilayer graphene thickness.

2 Theoretical Formulation

Figure 1 shows a schematic diagram of the proposed SPR substrate. A thin gold film with a thickness of 40 nm is coated on an SF10 glass prism and a dielectric SiO₂ layer is then deposited. Based on the Kretschmann configuration,^{16,17} p-polarized light at the wavelength $\lambda = 634$ nm illuminates the substrate. Contrary to the previous SPR-based detection of graphene layer number in water ambience,¹⁴ our substrate is designed in an air environment which can prevent any damage or contamination of the graphene samples during the experiments.

In particular we should emphasize that, since the resonance is determined at a higher angular position due to the presence of a thick SiO₂ layer, a prism with a higher refractive index is demanded to cover a wider angular range effectively. For example, if a BK7 prism is employed instead of SF10, the SPR angle is found at a value over 80 deg in an air environment and such a large SPR angle may cause several problems in practical measurement. Because a high

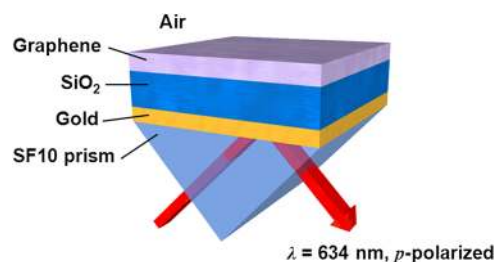


Fig. 1 Schematic of the proposed surface plasmon resonance (SPR) system with a dielectric overlayer. A 40-nm thick gold film is deposited on a high refractive index SF10 prism. Dielectric SiO₂ layer is deposited between gold film and graphene sheet. The superstrate is assumed as air and p-polarized light at $\lambda = 634$ nm is incident through the prism substrate.

refractive-index prism makes it possible to satisfy the phase-matching condition between the evanescent wave and the surface plasmons over a wide range of wave vectors by generating an evanescent wave with a large wave vector,¹⁸ the choice of SF10 rather than BK7 is appropriate for our SPR system. The relative permittivities $\epsilon = (n, k)$ of SF10 substrate and thin films of gold and SiO₂ are set to be (1.723, 0), (0.1857, 3.4182), and (1.457, 0), respectively, at $\lambda = 634$ nm.^{19,20} In our calculation, the homogeneous graphene layer is assumed to have an optical constant of $\epsilon = (2.889, 1.490)$ ²¹ and its thickness is equal to $d_{\text{graphene}} = L \times 0.335$ nm, where L is the number of graphene sheets.

A transfer-matrix method (TMM) is used to calculate the optical characteristics of our five-layer SPR system.²² The analytical solution of the reflectance R is represented by a 2×2 M -matrix, which is a serial product of the interface matrix I_{jk} ($j = 0, 1, 2, 3$, and $k = j + 1$) and the layer matrix L_j as follows:

$$R = \left| \frac{M_{12}}{M_{22}} \right|^2, \tag{1}$$

where

$$M = \begin{bmatrix} M_{11} & M_{12} \\ M_{21} & M_{22} \end{bmatrix} = I_{01}L_1L_{12}L_2L_{23}L_3L_{34}, \tag{2}$$

$$I_{jk} = \begin{bmatrix} 1 & r_{jk} \\ r_{jk} & 1 \end{bmatrix}, \tag{3}$$

$$L_j = \begin{bmatrix} e^{ik_{zj}d_j} & 0 \\ 0 & e^{ik_{zj}d_j} \end{bmatrix}. \tag{4}$$

Here, r_{jk} , k_{zj} , and d_j represent the Fresnel reflection coefficient wave vector in the z -direction, and the thickness of j 'th layer. r_{jk} and k_{zj} are given by

$$r_{jk} = \frac{\left(\frac{k_{zj}}{\epsilon_j} - \frac{k_{zk}}{\epsilon_k} \right)}{\left(\frac{k_{zj}}{\epsilon_j} + \frac{k_{zk}}{\epsilon_k} \right)}. \tag{5}$$

and

$$k_{zj} = \sqrt{\epsilon_j \left(\frac{\omega}{c} \right)^2 - k_x^2} \quad \text{with} \quad k_x = \sqrt{\epsilon_0} \frac{\omega}{c} \sin \theta_0, \tag{6}$$

where ω is the angular frequency, c is the speed of light in free space, and ϵ_0 is the relative permittivity of a prism substrate. The details of our TMM algorithm can be found elsewhere.²³

3 Results and Discussion

First of all, to optimize the SiO₂ thickness, we calculate the SPR angle shift, minimum reflectance at resonance (MRR), and SPR curve width when the SiO₂ thickness increases from 10 to 150 nm. The resonance shift value is determined by finding a change in SPR angles before and after introducing 10-nm thick graphene sheets whose layer number is 30. The SPR curve width obtained from the full width at half maximum (FWHM) and the MRR are calculated in the presence of the 10-nm thick graphene layer which uniformly covers the SiO₂ surface. As illustrated in Figs. 2(a) and 2(c), while we observe a maximum SPR shift of 11.1 deg at the SiO₂ thickness of 40 nm, it shows the highest FWHM of 19.1 deg and a relatively large MRR of 0.351. In general, as the FWHM and MRR are directly associated with the sensing contrast (i.e., the signal-to-noise ratio), such a weak SPR signal makes an accurate measure of the SPR angle less discriminating and thus, a deeper and narrower SPR dip is required. Figure 2(b) presents that the

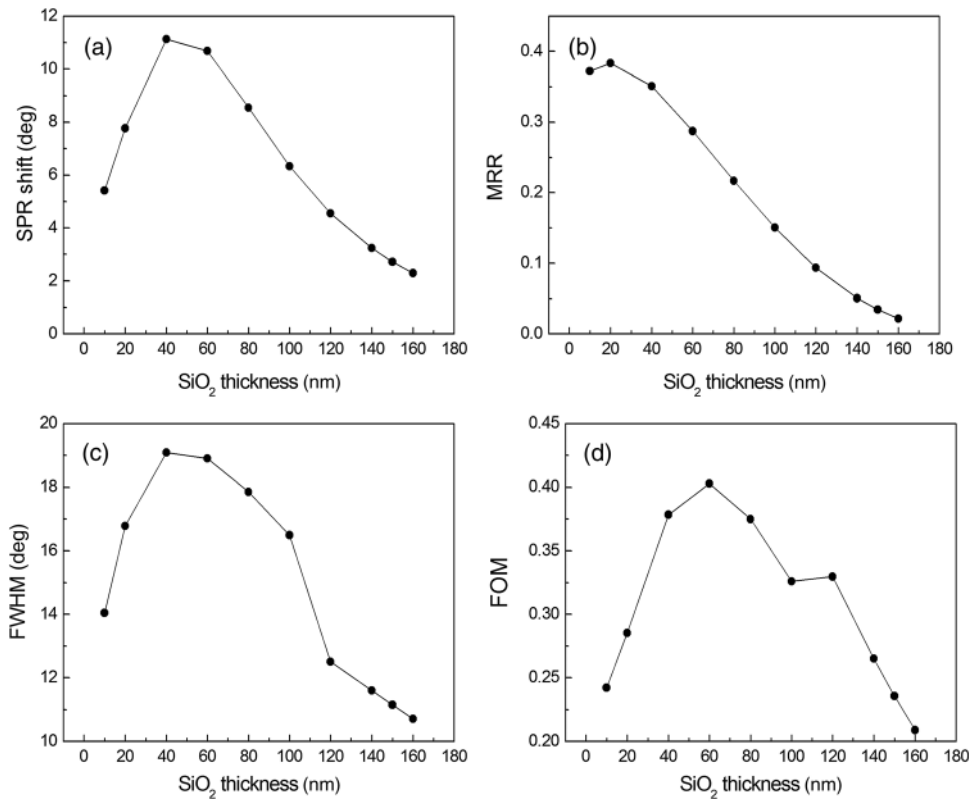


Fig. 2 Characteristics of (a) SPR angle shift, (b) minimum reflectance at resonance (MRR), (c) full width at half maximum (FWHM), and (d) figure of merit of the proposed SPR substrate as the SiO₂ layer thickness increases from 10 to 150 nm. The peak values of the resonance shift of 11.1 deg and the FWHM of 19.1 deg is found at the SiO₂ thickness of 40 nm. Also, a substantially decreasing trend in MRR is observed in accordance with an increase in SiO₂ thickness.

MRR is gradually decreasing with a growing SiO₂ thickness and this trend is consistent with our previous study on metal-dielectric double-layered plasmonic structures.¹⁵

Since the sensitivity, MRR, and FWHM have been used as important performance parameters of SPR detection, we introduce a figure of merit (FOM) to estimate an overall sensor performance quantitatively as

$$\text{FOM} = \frac{m[\text{deg}/\text{RIU}]}{\text{FWHM}[\text{deg}]} \cdot (1 - \text{MRR}), \quad (7)$$

where m is a shift of the resonance angle over the refractive-index range, which corresponds to the sensor sensitivity. Also, the FOM is a quality factor that considers both FWHM and MRR of the SPR curve. Hence, a smaller FWHM and a lower MRR are required for higher FOM because a deeper and narrower resonance dip allows efficient detection and precise analysis of sensing events.

From the FOM results in Fig. 2(d), while the peak FOM of 0.40 is found at the SiO₂ thickness of 60 nm, it has a large MRR of 0.287 and a wide FWHM of 18.9 deg. This implies that the highly broad and shallow curve is practically inappropriate for graphene layer discrimination. By assuming that the SPR curves with an MRR smaller than 0.2 are suitable for actual applications, the SiO₂ thickness of 120 nm can be suboptimal. This structure with FOM = 0.33 can provide a fairly good sensitivity, a low MRR of 0.094, and a narrow FWHM of 12.5 deg.

Next, using the optimized substrate structure, the reflectance characteristics of our SPR system are compared with the results based on a conventional SPR system consisting of four layers of BK7 prism, a 48-nm thick gold film, graphene sheets, and water ambience for small numbers of graphene layers.¹⁴ In Fig. 3, SPR curves of the two structures are calculated as a function of incidence angle. Strong absorption dips in both structures predict clear distinctions for different

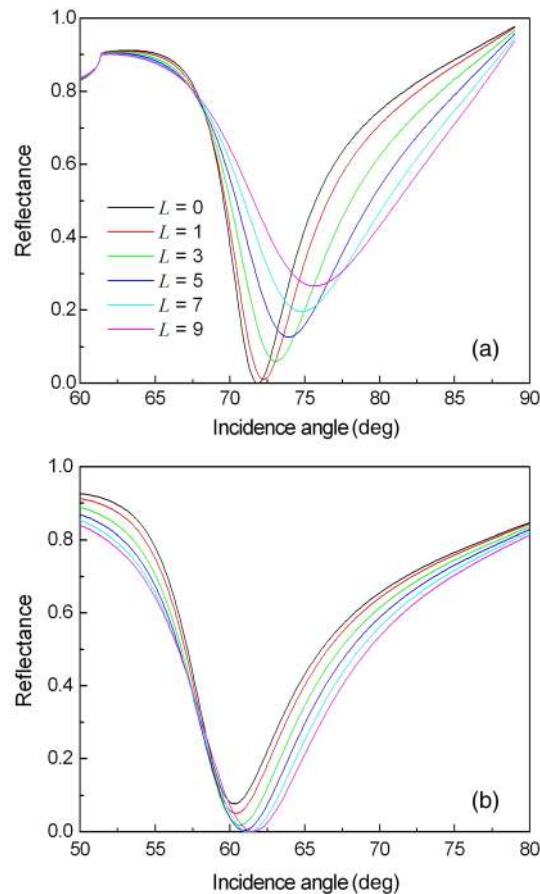


Fig. 3 SPR curves as a function of incidence angle for (a) the configuration presented in Ref. 16 and (b) the configuration shown in Fig. 1 when the graphene layer number L increases from 0 to 9. Note that the proposed SPR structure is computed in air ambience, while the conventional SPR system in (a) is covered with an aqueous solution.

graphene layer numbers and the SPR angles show a consistent increase with a growing L . In particular, one can see that the minimum reflectance for the conventional SPR system increases significantly with an increasing L , while the resonant absorption for the proposed SPR structure becomes stronger. Shallow SPR curves obtained from the conventional system are highly associated with the broadening of curve width, therefore deteriorating the resolution of the measurement and harming the low limit of detection.²⁴ For that reason, if we assume that the SPR curves with an MRR >0.2 are not practically available for accurate definition of the graphene layer number, the maximally detectable L can be determined to be 5 for the conventional SPR structure.

On the other hand, Fig. 4 demonstrates a three times enhancement in angular sensitivity for the conventional case. This improvement is attributed to an intense field-matter interaction in the vicinity of the gold surface, namely, overlap integral within the ambience region.²⁵ However, as it is no longer persuasive for a larger graphene thickness due to a broad and shallow SPR curve, the advantage of the proposed substrate incorporating SiO₂ layer seems prominent at this thickness range of $L > 5$. Moreover, during the measurement, our configuration in air ambience is essentially free from any damages caused by an attachment of flow channel or container for aqueous solutions.

Subsequently, the proposed SPR substrate is applied to detect a significant number of graphene layers of $L \geq 10$. Although we find a slight growth of minimum reflectance in accordance with L for the proposed structure in Fig. 5, the MRR does not exceed 0.1 even at $L = 20$, and the value is still smaller than 0.2 up to $L = 50$. Since the propagating surface plasmon waves are less interfered with a graphene sheet due to the presence of an SiO₂ overlayer, an effective excitation

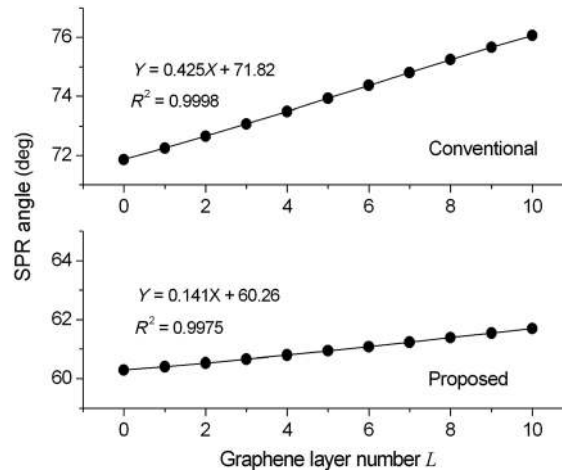


Fig. 4 Linear regression analyses between the resonance angle and the graphene layer number L for the conventional and the proposed SPR structures. At this range of graphene number, the SPR angle shift shows a high linearity in both cases.

of resonant plasmon may induce a strong absorption dip at the resonance. On the other hand, while the results are not shown here, a remarkable increase in MRR over the range of L is observed for the conventional one. In addition, Fig. 6 presents a linear regression analysis between the SPR angle and the graphene layer number. We note that the SPR angle linearly increases until L reaches 50, but its slope becomes slowly decreased beyond this range. Summarizing the results in Figs. 5 and 6, the accuracy and linearity in SPR detection can be guaranteed in a wide range of graphene layer numbers and the maximally detectable L is found to be 50 for the proposed SPR structure with a 120-nm thick SiO_2 layer.

In order to verify the effect of a dielectric spacer between the gold film and graphene sheet, we visualize the distribution of plasmon field intensity near the gold surface using the finite difference time domain (FDTD) method. For a comparison study, we have chosen the conventional and the proposed SPR substrates with and without a 10-nm thick graphene layer. Also, we assume that the illumination of $\lambda = 634$ nm has a resonance angle determined by TMM calculation and the minimum grid size is set to be 0.5 nm. In Fig. 7(a), the FDTD calculation exhibits well-known features of surface plasmon modes. Surface-enhanced electromagnetic fields are exponentially decreased along the distance from a gold film. On the assumption that the field of an incident beam is of unit intensity, maximum E_x field is found at the gold surface and its intensity is obtained as 24.5 for the conventional SPR scheme and 16.3 for the proposed

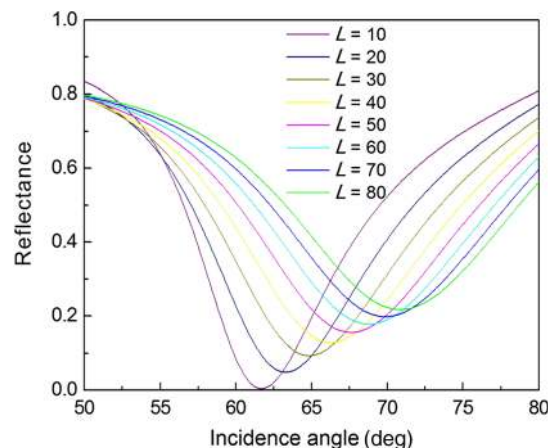


Fig. 5 SPR curves as a function of incidence angle for the configuration shown in Fig. 1 when the graphene layer number L increases from 10 to 80.

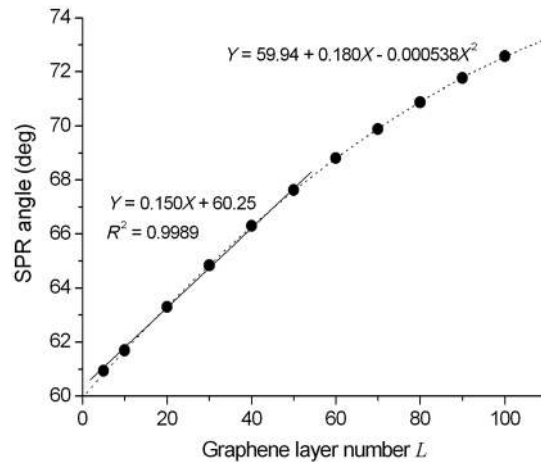


Fig. 6 Linear regression analysis (solid line) and second-order polynomial fit (dotted line) between the SPR angle and the graphene layer number. The SPR angle linearly increases in the range of $L \leq 50$, but its slope becomes slowly decreased beyond this range.

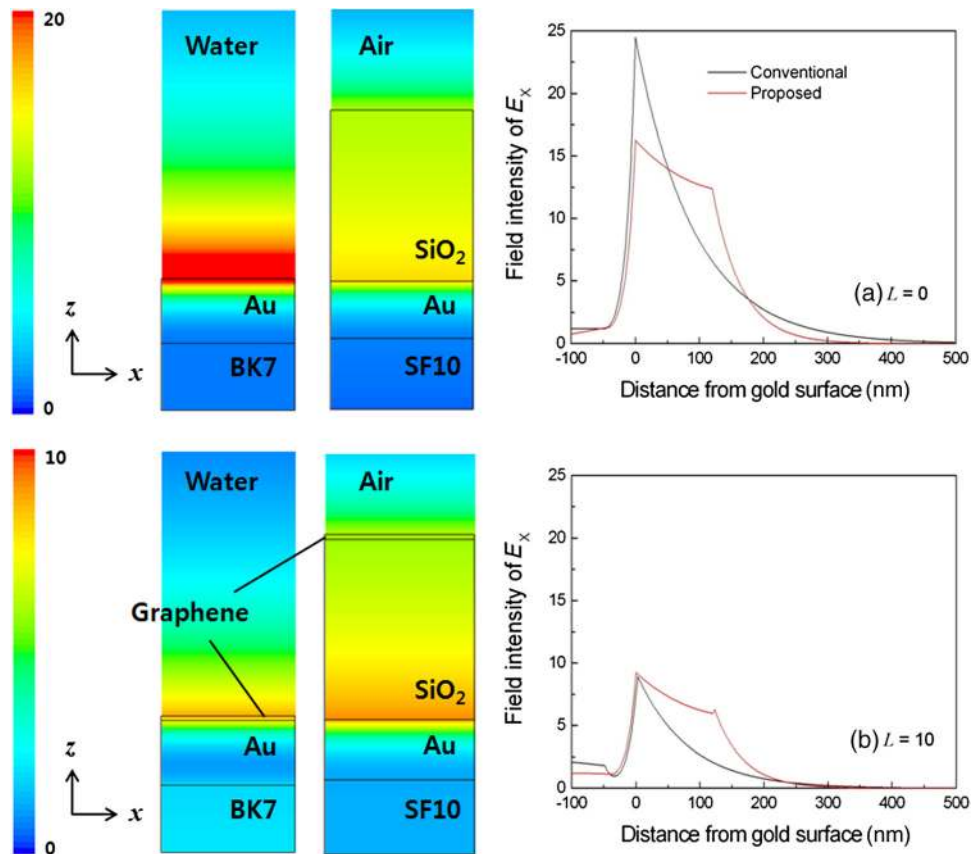


Fig. 7 Horizontal field intensity distributions of E_x for the conventional and the proposed SPR structures when (a) $L = 0$ and (b) $L = 10$. For $L = 0$, the incidence angles are 71.86 deg for the conventional and 60.30 deg for the proposed SPR schemes and the two-dimensional images obtained from the FDTD calculations are normalized by the field intensity of 20. On the other hand, for $L = 10$, the incidence angles are 76.06 and 61.70 deg, respectively, and the FDTD images are normalized by the field intensity of 10.

one when no graphene sheet is applied. On top of the SiO₂ layer where the graphene will be attached, peak plasmon field intensity is found to be 12.4 and the contrast in field intensity at the surface exposed to graphene makes the conventional scheme more sensitive as shown in Fig. 4. When 10 graphene layers are deposited on the two SPR structures in Fig. 7(b), the peak intensity of the conventional system is $E_x = 8.9$, while the suggested one produces a larger peak of $E_x = 9.3$. From the FDTD results, we find that the SiO₂-gold substrate plays a significant role in reducing a direct destructive interplay between the propagating plasmon waves and absorptive graphene sheets. Another important aspect is that, due to a strong overlap of the absorbed matter with the excited surface plasmons in the vicinity of gold film, attachment of a thick graphene sheet may contribute to a distortion of dispersion relation, inevitably leading to a shallow and broad SPR curve.

The main advantage of the proposed SPR substrate with a dielectric overlayer is that it allows for a nonintrusive and real-time counting of thick graphene layers. However, we need to emphasize that such a wide dynamic range in thickness determination is realized at the expense of sensitivity in measurement. It is well known in SPR sensor studies that there is a trade-off between the detection sensitivity and the SPR curve characteristic.²⁶ In this regard, a brief discussion on the detection limit depending on the sensitivity and the standard deviation (SD) will be helpful for future experimental works. In general, the detection limit is expressed as $3 \times \text{SD}/m$. As the sensitivity of the suggested SPR scheme is theoretically determined to be 0.150 deg/L, the SD value should be <0.05 deg for accurate graphene thickness measure. Based on our previous studies on the thin-film-based SPR structures, the SD values did not exceed 0.03 deg experimentally^{27,28} and this can guarantee the effectiveness of our suggestion. However, to satisfy this condition by a wide margin, we may employ a rotation stage with enhanced angular resolution or use a more powerful laser source with a sensitive detector. Also, careful attention should be paid to the surface roughness during the fabrication process of the SiO₂ layer and multilayer graphene sheet.

4 Conclusion

In summary, we have explored a modified SPR substrate including an SiO₂ layer to provide the accuracy and reliability in counting the multilayer graphene sheets. The proposed structure confirms a fairly good sensitivity as well as a greatly improved reflectance curve compared with a conventional SPR scheme. Also, in contrast to the previous optical attempts including Raman signal and the relative reflectance and transmittance change, our suggestion shows several unique advantages, e.g., a high linearity in a wide range of graphene layer numbers. From our theoretical study, we find that the SiO₂ layer plays an important role in achieving such an improvement by preventing the excited plasmons from being highly degenerated. An optimal SiO₂ layer on a gold film allows the maximally countable graphene layer number to reach up to 50 from linear regression analysis. Although transferring the target graphene material to plasmonic substrates of a metal/oxide combination in a simple and reproducible manner still remains a challenge, it is hoped that the proposed SPR structure could offer a new possibility for non-intrusive, fast, and reliable SPR detection of the graphene layer thickness.

Acknowledgments

Under K.M.B.'s supervision, S.H.E. calculated SPR characteristics of the suggested structures based on transfer-matrix method and wrote the article. N.H.K. obtained the near-field distributions using FDTD simulation. This work was supported by the National Research Foundation of Korea (NRF) grant funded by the Korea Government (MEST) (2011-0029485).

References

1. A. H. C. Neto et al., "The electronic properties of graphene," *Rev. Mod. Phys.* **81**(1), 109–162 (2009).

2. K. S. Novoselov et al., "Electric field effect in atomically thin carbon films," *Science* **306**(5696), 666–669 (2004).
3. S. Y. Shin et al., "Control of the π plasmon in a single layer graphene by charge doping," *Appl. Phys. Lett.* **99**(8), 082110 (2011).
4. O. Salihoglu, S. Balci, and C. Kocabas, "Plasmon-polaritons on graphene-metal surface and their use in biosensors," *Appl. Phys. Lett.* **100**(21), 213110 (2012).
5. S. H. Choi, Y. L. Kim, and K. M. Byun, "Graphene-on-silver substrates for sensitive surface plasmon resonance imaging biosensors," *Opt. Express* **19**(2), 458–466 (2011).
6. D. E. Jiang, V. R. Cooper, and S. Dai, "Porous graphene as the ultimate membrane for gas separation," *Nano Lett.* **9**(12), 4019–4024 (2009).
7. Y. Sui and J. Appenzeller, "Screening and interlayer coupling in multilayer graphene field-effect transistors," *Nano Lett.* **9**(8), 2973–2977 (2009).
8. S. Zhao, Y. Lv, and X. Yang, "Layer-dependent nanoscale electrical properties of graphene studied by conductive scanning probe microscopy," *Nanoscale Res. Lett.* **6**(1), 498 (2011).
9. Z. Ni et al., "Raman spectroscopy and imaging of graphene," *Nano Res.* **1**(4), 273–291 (2008).
10. A. C. Ferrari et al., "Raman spectrum of graphene and graphene layers," *Phys. Rev. Lett.* **97**(18), 187401 (2006).
11. D. Yoon et al., "Interference effect on Raman spectrum of graphene on SiO₂/Si," *Phys. Rev. B* **80**(12), 125422 (2009).
12. C. Casiraghi et al., "Raman fingerprint of charged impurities in graphene," *Appl. Phys. Lett.* **91**(23), 233108 (2007).
13. W. Zhu et al., "Layer number determination and thickness-dependent properties of graphene grown on SiC," *IEEE Trans. Nanotechnol.* **10**(5), 1196–1201 (2011).
14. S. Cheon et al., "How to optically count graphene layers," *Opt. Lett.* **37**(18), 3765–3767 (2012).
15. S. M. Jang et al., "Enhancement of localized surface plasmon resonance detection by incorporating metal-dielectric double-layered subwavelength gratings," *Appl. Opt.* **50**(18), 2846–2854 (2011).
16. T. Turbadar, "Complete absorption of light by thin metal films," *Proc. Phys. Soc.* **73**(1), 40–44 (1959).
17. E. Kretschmann, "Decay of non radiative surface plasmons into light on rough silver films: comparison of experimental and theoretical results," *Opt. Commun.* **6**(2), 185–187 (1972).
18. C. H. Park, J. W. Choi, and Y.-H. Cho, "Real-time surface plasmon resonance dispersion imaging with a wide range of incident angles and detection wavelengths," *Appl. Opt.* **49**(13), 2470–2474 (2010).
19. P. B. Johnson and R. W. Christy, "Optical constants of the noble metals," *Phys. Rev. B* **6**(12), 4370–4379 (1972).
20. E. D. Palik, *Handbook of Optical Constants of Solids*, Academic Press, New York (1985).
21. M. Klintonberg et al., "Evolving properties of two dimensional materials from graphene to graphite," *J. Phys.: Condens. Matter* **21**(33), 335502 (2009).
22. A. Yariv and P. Yeh, *Optical Waves in Crystals: Propagation and Control of Laser Radiation*, Wiley, New York (1984).
23. S. H. Choi and K. M. Byun, "Investigation on an application of silver substrates for sensitive surface plasmon resonance imaging detection," *J. Opt. Soc. Am. A* **27**(10), 2229–2236 (2010).
24. A. Shalabney and I. Abdulhalim, "Figure-of-merit enhancement of surface plasmon resonance sensors in the spectral interrogation," *Opt. Lett.* **37**(7), 1175–1177 (2012).
25. A. Shalabney and I. Abdulhalim, "Electromagnetic fields distribution in multilayer thin film structures and the origin of sensitivity enhancement in surface plasmon resonance sensors," *Sens. Actuators A* **159**(1), 24–32 (2010).
26. K. M. Byun, M. L. Shuler, S. J. Kim, S. J. Yoon, and D. Kim, "Sensitivity enhancement of surface plasmon resonance imaging using periodic metallic nanowires," *J. Lightwave Technol.* **26**(11), 1472–1478 (2008).

27. K. M. Byun et al., "Enhanced surface plasmon resonance detection using porous ITO-gold hybrid substrates," *Appl. Phys. B: Lasers Opt.* **107**(3), 803–808 (2012).
28. K. M. Byun et al., "Experimental study of sensitivity enhancement in surface plasmon resonance biosensors by use of periodic metallic nanowires," *Opt. Lett.* **32**(13), 1902–1904 (2007).



Sherif H. El-Gohary received BS and MS degrees in the Department of Biomedical Engineering from Cairo University, Cairo, Egypt, in 2005 and 2009, respectively. He joined Kyung Hee University, Yongin, Korea, in 2012. Since 2005, he has been with the School of Engineering, Cairo University, where he works as a teaching lecturer. His main areas of research interest are high-sensitivity plasmonic biosensors with metallic nanostructures and theoretical studies on tissue-light interactions.



Nak-Hyeon Kim received a BS degree in the Department of Biomedical Engineering from Kunkuk University, Chungju, Korea, in 2009. Since then, he joined the Department of Biomedical Engineering, Kyung Hee University, Yongin, Korea and has been working under combined master's and doctorate program. His main area of research interest is an ultra-sensitive detection of biomolecular interactions based on SPR technique.



Kyung Min Byun received BS and MS degrees from the School of Electrical Engineering, Seoul National University, Seoul, Korea, and the PhD degree from Seoul National University, in 2007. From July 2007 to February 2008, he worked as a visiting scientist in the Department of Biomedical Engineering, Cornell University, Ithaca, NY. He is currently an assistant professor at the Department of Biomedical Engineering, Kyung Hee University, Yongin, Korea. His main research activities include theoretical and experimental studies on highly sensitive localized SPR biosensors, optical detection and stimulation of neural signals, and photo-acoustic imaging technique.